

Development of the superconducting squeezed elliptical cavity with $b=0.81$ for the Fermilab Proton Driver. First results.

I.Gonin, T.Khabiboulline, N.Solyak

Abstract: Proton Driver needs different types of accelerating cavities to accelerate protons from 15 MeV to 8 GeV. Here we present the preliminary design of the superconducting elliptical $b=0.81$ cavity for beam acceleration in range 400-1200 MeV.

1. General layout

Accelerating Linac for the Proton Driver consists of different types of cavities as shown on Fig.1. The medium energy part of the linac (15 - 408 MeV) consists of three types of 325 MHz superconducting spoke resonators: single spoke (SSR), double spoke (DSR) and triple spoke (TSR). High energy part of the PD linac is built from two types of SC 1.3 GHz elliptical cavities: squeezed ($\beta = 0.81$) and TESLA ($\beta = 1$) cavities. Scheme of the linac and general parameters of the SC cavities are shown in picture and table below [1].

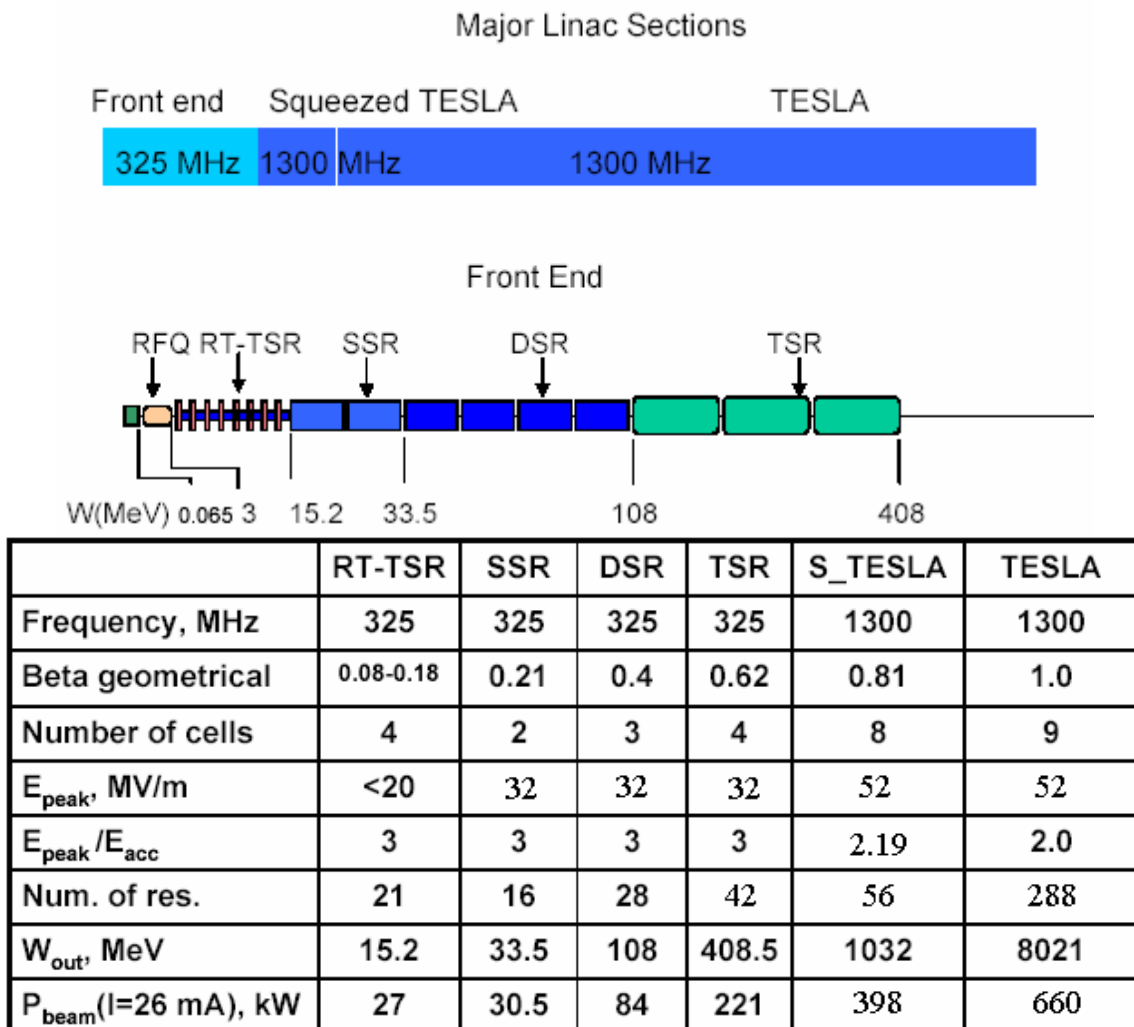


Fig.1. General layout of the Proton Driver and the Table of parameters for SC cavities.

2. Short (6-cell) vs. Long (8-cell) cavity.

For the PD SC cavities we suppose that the maximum surface field not exceeds fields in TESLA with 26 MV/m accelerating gradient. This level can be reliably achieved with existing state-of-art technology of superconducting cavities. Corresponding maximum value of surface fields are: $E_{peak} = 52 \text{ MV/m}$ and $H_{peak} = 111 \text{ mT}$. In Fig.2 the energy gain per cavity for different types of SC resonators are calculated (accelerating in crest was assumed). Fig.3 shows comparison 6-cell and 8-cell cavities, both at with 52 MV/m surface peak electric fields and -30 degrees beam out of crest phase.

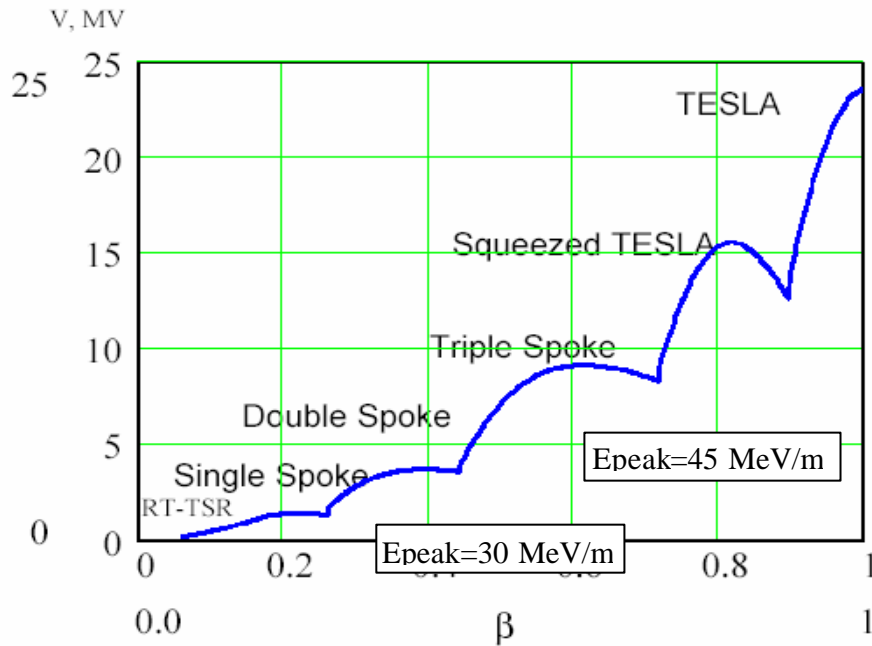


Fig.2. Energy gain in cavity vs. $\beta=v/c$. Here we assume acceleration on the crest.

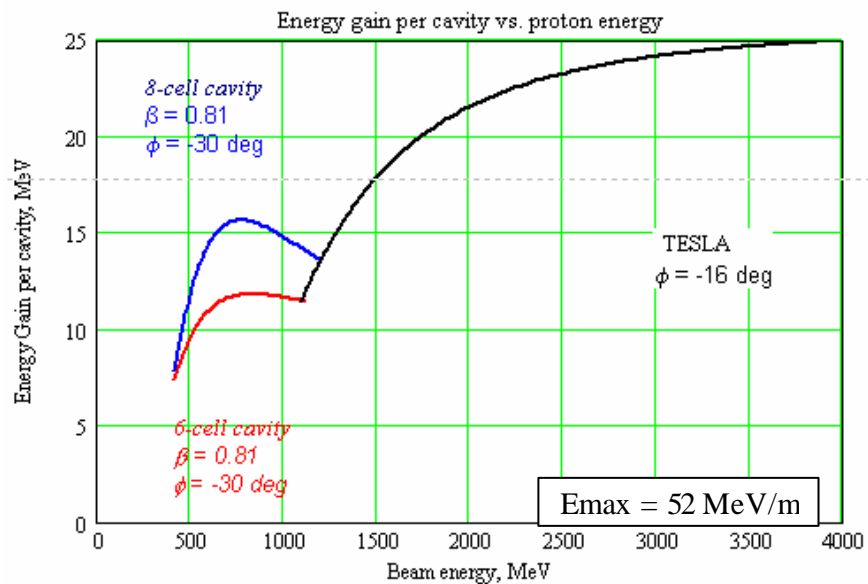


Fig.3. Energy gain per cavity vs. proton energy. Acceleration out of crest phase is included.

Long cavity option is more cost effective and will allow save ~10 cavities (including power couplers, phase shifters etc) or 2 cryomodules. Number of cavities needed and transition energy (from squeezed to TESLA cavities) are shown below.

E _{max} = 52 MeV/m	N6 := 64	N_TESLA := 292	W_trans := 110C
	N8 := 56	N_TESLA := 288	W_trans := 119C

3. SNS-like cavity.

For the geometry of the squeezed cavity we consider two choices. The first one is SNS like design, scaled from 805 MHz to 1300MHz. The general parameters and geometry of the 6-cell cavity are shown in Fig. 4. By adding two more mid-cells this cavity can be extended to 8-cell cavity. In this case R/Q will be increased proportionally to cavity length.

The $\beta_g = 0.81$ Cavity for SNS / PD

Effective β that matches the TTF curve = 0.810

E _p /E _{acc}	2.19 (2.14 inner cell)
B _p /E _{acc} [mT/(MV/m)]	4.79 (4.58 inner cell)
R/Q [Ω]	484.8
G [Ω]	233
k [%]	1.52
Q _{BCS} @ 2 K [10 ⁹]	36.2 / 13.9
Frequency [MHz]	805 / 1300
Field Flatness [%]	1.1

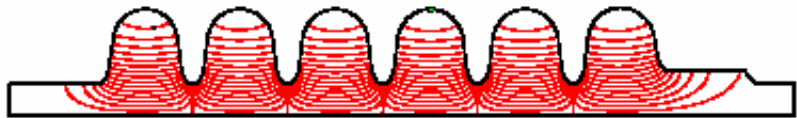


Fig.4. The general parameters scaled from SNS 6-cell cavity

The geometrical parameters of the squeezed 1.3GHz cavity are shown on the table below. The used in table parameters are explained in Fig.5

	Geometrical Parameters		
	Inner cell	End Cell Left	End Group (coupler) Left Right
L [mm]	46.75	46.75	46.75
R _{iris} [mm]	30.22	30.22	30.22 43.35
D [mm]	101.65	101.65	102.86
d [mm]	9.29	8.05	9.29 8.05
r	1.8	1.6	1.8 1.6
R	1.0	1.0	1.0
α [deg]	7.0	10.072	7.0 10.0

Cell Shape Parametrization

- Full parametric model of the cavity in terms of 7 meaningful geometrical parameters:
 - ✓ Ellipse ratio at the equator ($R=B/A$)
Ruled by Mechanics
 - ✓ Ellipse ratio at the iris ($r=b/a$)
Epeak
 - ✓ Side wall inclination (α) and position (d)
Epeak vs. Bpeak tradeoff and coupling k
 - ✓ Cavity iris radius R_{iris}
Coupling k
 - ✓ Cavity Length L
 β
 - ✓ Cavity radius D
used for frequency tuning
- Behavior of all e.m. and mechanical properties has been found as a function of the above parameters

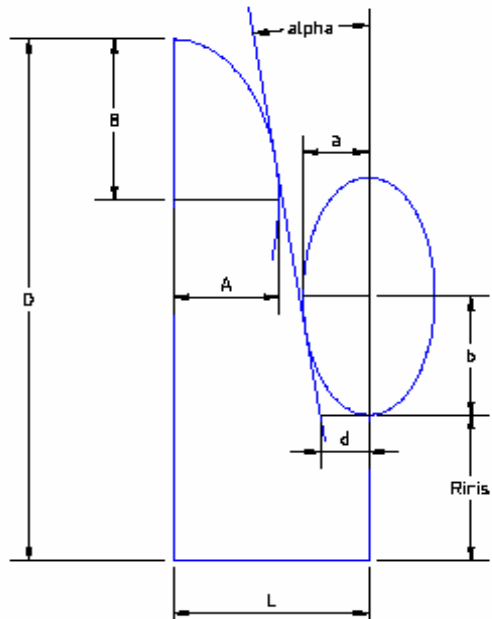


Fig. 5. Cell shape parametrization.

4. Low Losses 8-cell Cavity.

The second choice is new optimized design for 8-cell cavity. The goal of optimization was to reduce H_{peak}/E_{acc} ratio, which allow us minimize the power losses in cavity, or for the same surface magnetic field, increase acceleration gradient. The diameter of the end-tube was chosen the same as for TESLA cavity. In this case we can use the same TESLA design of the end-groups, including HOM couplers, main coupler, antenna and conical flanges (see Fig.6). The only difference is the cell geometry.

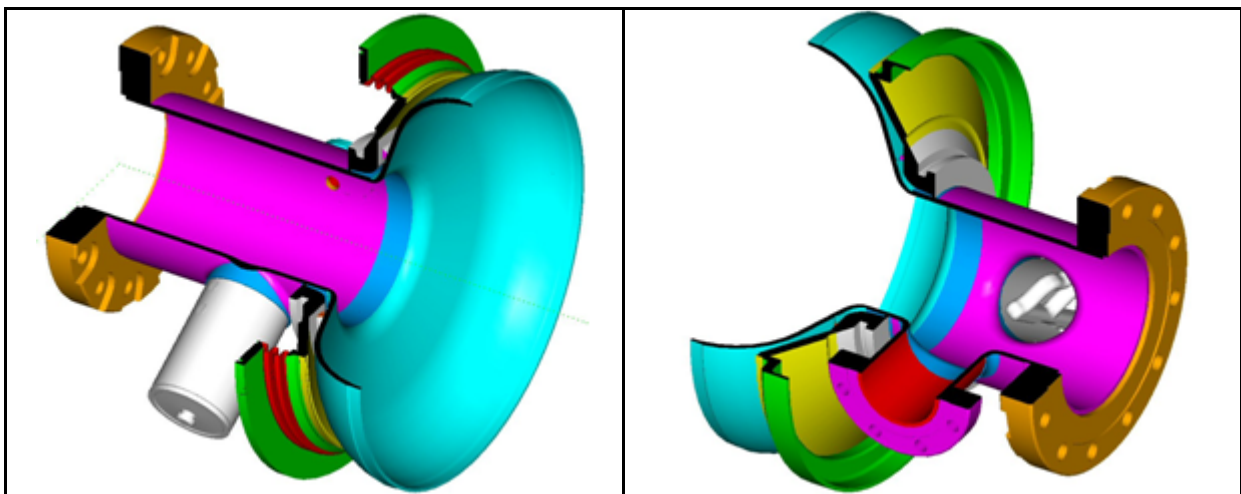


Fig.6. Squeezed TESLA cavity end-group assemblies are the same as TESLA cavity except end-cell geometry

The playing parameters for the mid-cell optimization are wall inclination angle (α) and ellipse ratios at the iris and equator (see Fig.5). Iris radius was fixed 30mm, the equator radius was defined by working frequency. As a reference point for the comparison the SNS-like geometry was used. The decreasing of the inclination angle will redistribute magnetic field along the bigger surface, which cause reduction of the peak magnetic field and increasing of shunt impedance and geometrical factor. It also increases cell-to-cell coupling and even rigidity of the cavity. Only one parameters become worse – the surface electric field, but experience of the DESY shows that the cavity performances are not limited by electric field if appropriate surface preparation is applied (high pressure water rinsing, clean assembly, etc) . The main parameters of the cavity are shown for two inclination angles vs. ellipse ratio at equator is shown in Fig.7. All parameters are normalized to the parameters of SNS-like cavity (see Fig.4).

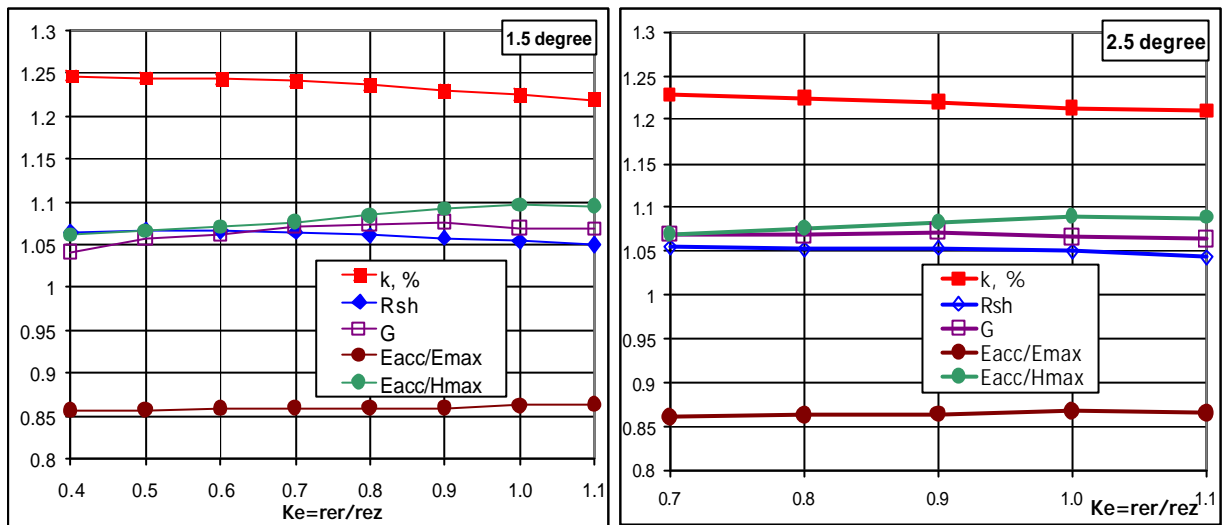
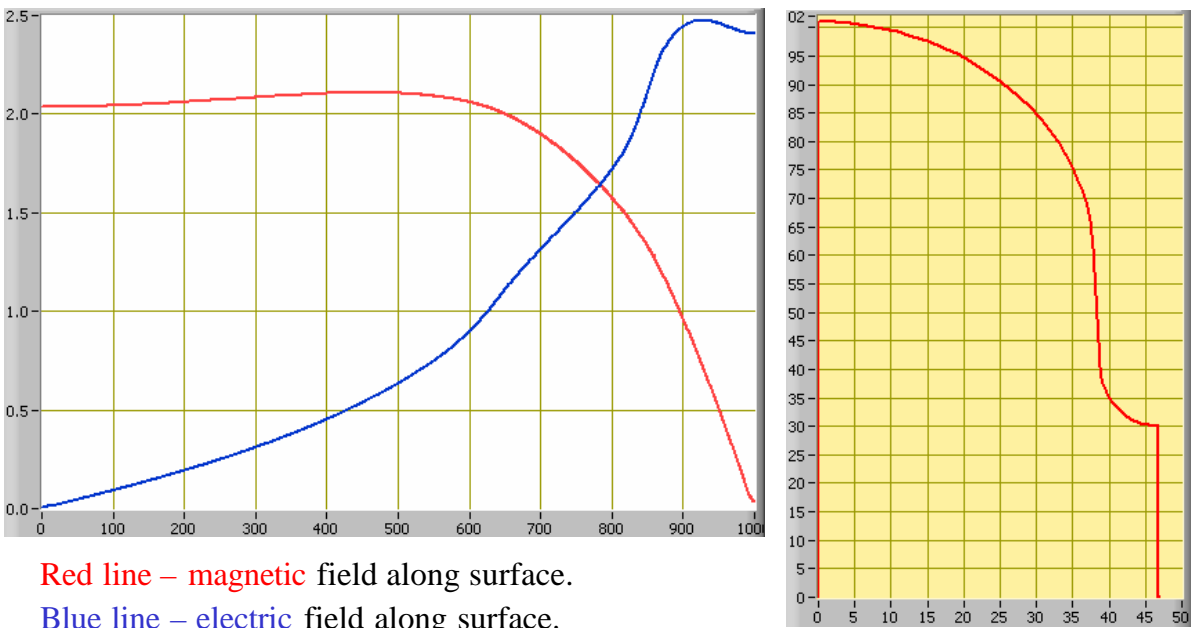


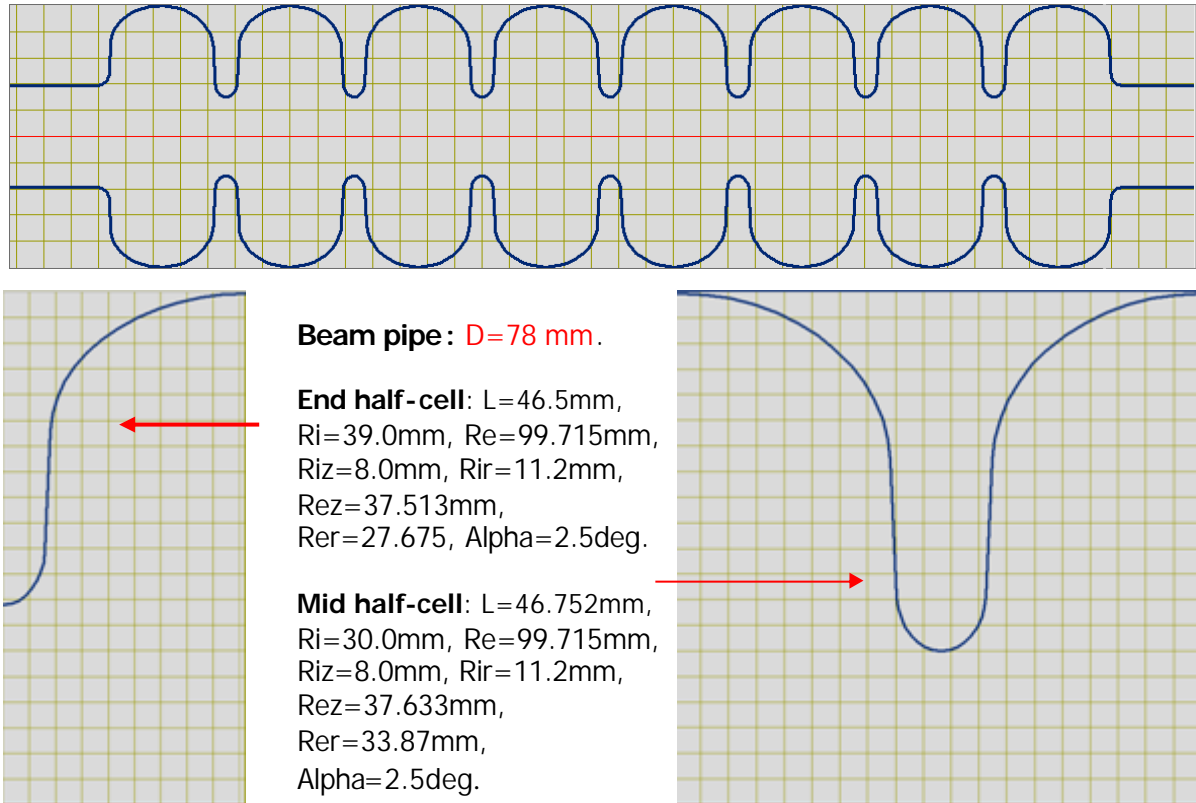
Fig.7. Normalized cavity parameters vs. ellipse ratio at cell equator.



Red line – magnetic field along surface.
Blue line – electric field along surface.

Fig.8. Electric and magnetic field distribution along surface (arbitrary units).

The chosen geometry of the cavity and main parameters are shown in Fig.9. As one can see the magnetic field in this geometry is ~10% lower than for SNS-like design for the same accelerating gradient. The TESLA cavity parameters are shown in the table for comparison. The field profile in the mid-cell is shown in Fig.8.



Geometrical Beta of Sections	0.81	1
RF frequency (MHz)	1300	1300
Cavity Type	FNAL	TTF
Number of Cells Per Cavity	8	9
Cell-to-Cell Coupling Constant	0.018	0.0187
Unloaded Q_0	$>5E9$	$>1E10$
External Q	700000	1500000
External Q Variation	+/- 20%	+/- 20%
R/ Q_0 (function of beam velocity)	674	1036
Cavity Active Length (geometrical)	0.74718	1.03774
Cavity Total Length incl. Couplers	0.96718	1.25774
Cavity Slot Length incl. avg. Bellows	1.03218	1.32274
Iris Diameter	60	70
Beam pipe Diameter	78	78
ID at Equator	199.43	206
E_{peak} (max)	58.6484	52
$B_{\text{peak}}/E_{\text{acc}}$	4.33	4.26
B_{peak}	102.813	110.76
$E_{\text{peak}}/E_{\text{acc}}$	2.47	2
E_{acc} (max, on crest for Beta-design)	23.74	26

Fig.9. Cavity dimensions and main parameters optimized for Low Losses.

4.1. Monopole Modes in LL squeezed cavity.

The dispersive diagram for the monopole modes and the plot of the R/Q for 8-cell cavity are shown in Fig.10. The table below presents (R/Q) value for the first few passbands. Dotted line corresponds the proton beam with $\beta=0.81$. The maximum R/Q correspond working frequency 1300 MHz.

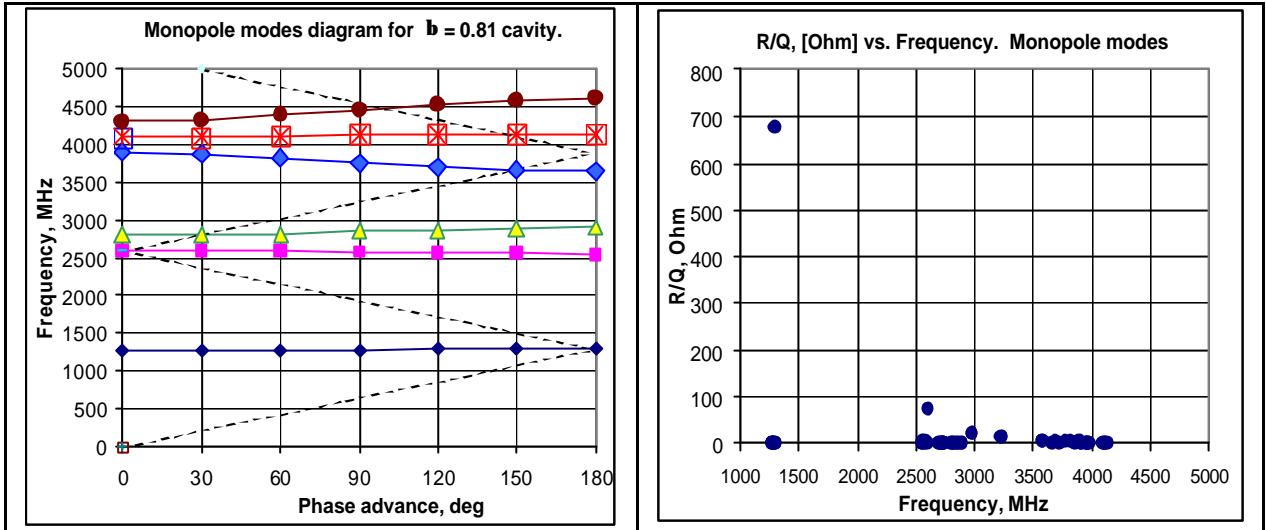


Fig.10. Dispersive diagram of the mid-cell (left) and R/Q vs. frequency (right) for monopole modes

M0		M1		M2		M3		M4		M5		M6	
MHz	R/Q	MHz	R/Q	MHz	R/Q	MHz	R/Q	MHz	R/Q	MHz	R/Q	MHz	R/Q
1277.7	0.00	2551.3	0.05	2804.8	0.04	2980.3	20.37	3729.2	0.05	3955.0	0.00	4120.6	0.04
1280.3	0.06	2552.2	2.04	2809.5	0.00	2981.0	20.41	3774.7	1.74	3957.9	0.00	4127.6	0.02
1284.2	0.05	2557.8	0.03	2819.5	0.53	3231.8	15.24	3821.6	3.00	3961.8	0.00	4131.9	0.04
1288.8	0.21	2565.8	2.11	2834.1	0.32	3235.4	15.13	3863.4	0.45	3966.3	0.00	4134.4	0.72
1293.4	0.10	2575.7	0.02	2851.7	0.01	3575.9	5.90	3893.0	2.62	3970.4	0.00	4135.8	1.53
1297.2	0.31	2586.3	6.72	2869.8	0.18	3580.5	4.80	3906.4	1.77	3973.3	0.00	4136.1	0.19
1299.8	0.34	2595.9	0.01	2885.7	0.02	3662.6	0.27	3914.3	0.00	4103.5	0.11	4214.2	0.00
1300.8	673.93	2602.6	75.09	2896.7	0.02	3690.1	3.26	3914.5	0.00	4111.4	0.07	4214.5	0.00

Table 1: R/Q (Ohm) for the first few monopole passbands.

4.2. Dipole High Order Modes.

Dispersion diagram for the dipole modes, calculated for mid-cell geometry is shown in Fig.12 (plot on the left). One can see that only 1st and 3^d passbands are narrow, that means that we can expect highest R/Q for these modes. Right plot in Fig.12 shows R/Q value vs. frequency calculated for full 8-cell cavity. Electric field distribution

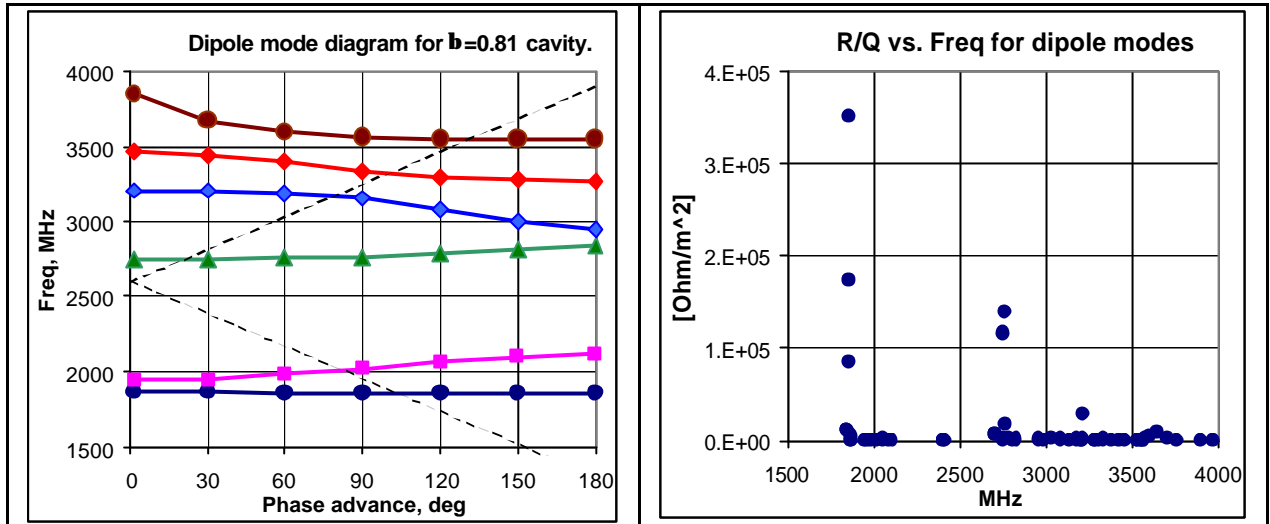


Fig. 11. Dispersive diagram of the mid-cell (left) and R/Q vs. frequency (right) for dipole modes

M0		M1		M2		M3		M4		M5		M6		M7	
MHz	R/Q	MHz	R/Q	MHz	R/Q	MHz	R/Q	MHz	R/Q	MHz	R/Q	MHz	R/Q	MHz	R/Q
1277.7	0.00	2551.3	0.05	2804.8	0.04	2980.3	20.37	3729.2	0.05	3955.0	0.00	4120.6	0.04	4236.4	4.71
1280.3	0.06	2552.2	2.04	2809.5	0.00	2981.0	20.41	3774.7	1.74	3957.9	0.00	4127.6	0.02	4244.7	4.84
1284.2	0.05	2557.8	0.03	2819.5	0.53	3231.8	15.24	3821.6	3.00	3961.8	0.00	4131.9	0.04	4299.2	0.00
1288.8	0.21	2565.8	2.11	2834.1	0.32	3235.4	15.13	3863.4	0.45	3966.3	0.00	4134.4	0.72	4305.7	0.00
1293.4	0.10	2575.7	0.02	2851.7	0.01	3575.9	5.90	3893.0	2.62	3970.4	0.00	4135.8	1.53	4314.4	0.00
1297.2	0.31	2586.3	6.72	2869.8	0.18	3580.5	4.80	3906.4	1.77	3973.3	0.00	4136.1	0.19	4323.7	0.00
1299.8	0.34	2595.9	0.01	2885.7	0.02	3662.6	0.27	3914.3	0.00	4103.5	0.11	4214.2	0.00	4327.5	0.43
1300.8	673.93	2602.6	75.09	2896.7	0.02	3690.1	3.26	3914.5	0.00	4111.4	0.07	4214.5	0.00	4331.6	0.00

Table.2. (R/Q) [Ohm/m^2] for different passbands

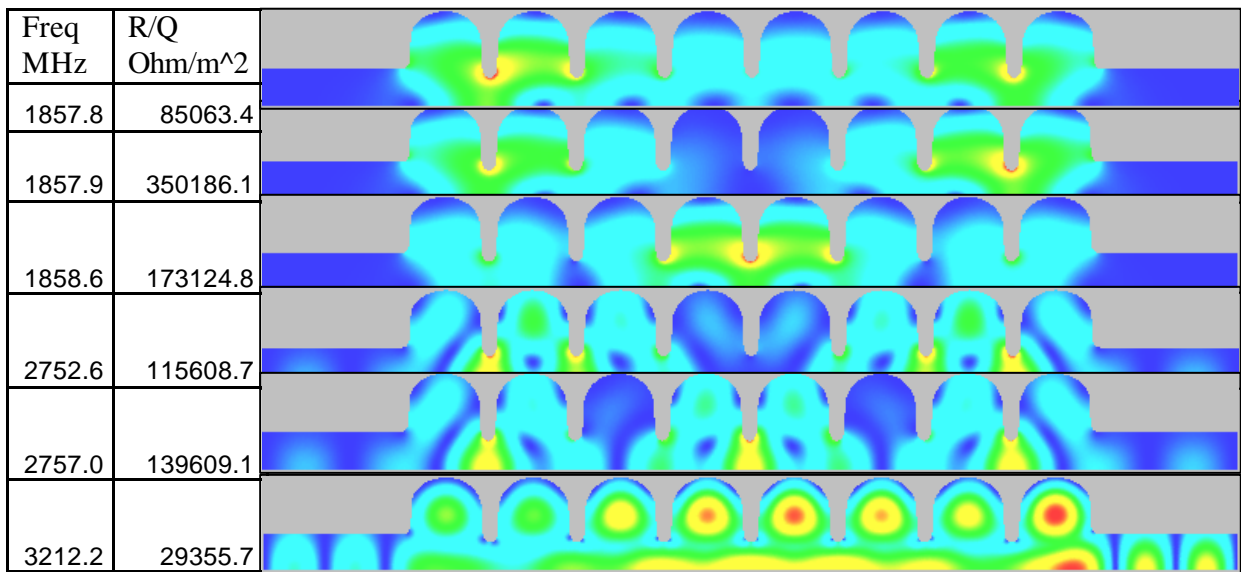


Fig.12. E-field pattern for dipole HOMs with the highest R/Q.

4.3. Lorentz Forces and Detuning

Lorentz forces were simulated by ANSYS for the regular mid-cell with the fixed longitudinally at the irises. As known from simulations of the Lorentz detuning for the TESLA cavity these boundary conditions provide good agreement with the experimental data. Electromagnetic pressure distribution along the surface of the mid-cell is shown in Fig.13 on the left. Pressure is negative for electric field and positive for magnetic field. The picture of the surface displacement due to Lorentz forces, simulated for $E_{acc}=25$ MV/m is plotted on right. Both electric and magnetic fields detune cavity in the same direction.

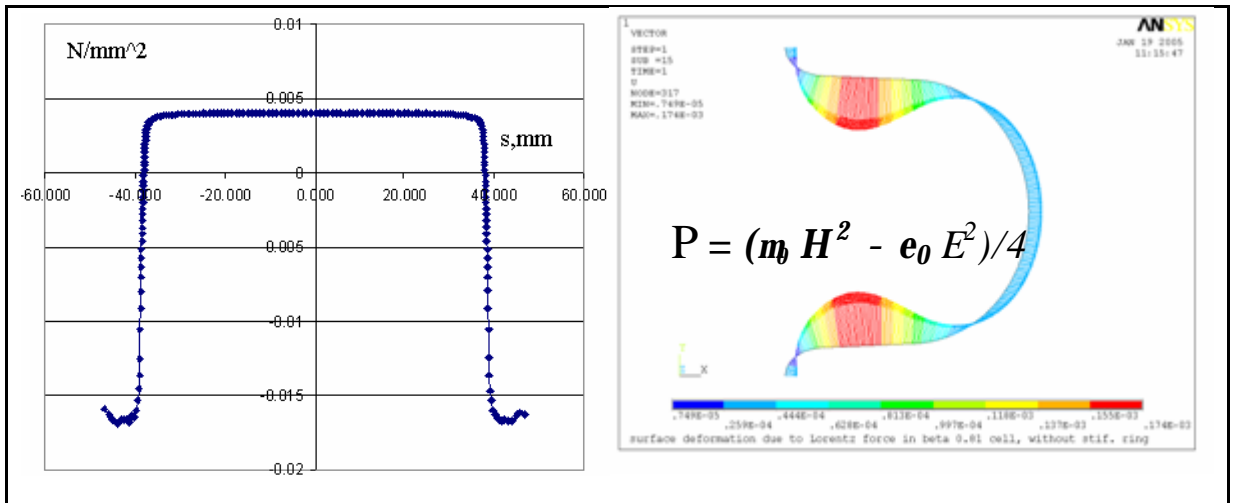


Fig.13. Pressure distribution along the cavity (left) and vector of displacement in the cavity (right).

Cavity detuning can be reduced by stiffening rings as it was done in TESLA cavity. The position of ring was optimized to get the minimum detuning. The result of optimization is shown in Fig.14 (left) where detuning coefficient KL is plotted vs. position of stiffening ring. The minimum detuning will be for 42.5mm. Thickness of ring is equal 3 mm the same as thickness of niobium used for cavity production. The increasing of the wall thickness reduces Lorentz detuning almost linearly (Fig.14 on right). The stiffening ring in simulation was in optimum position.

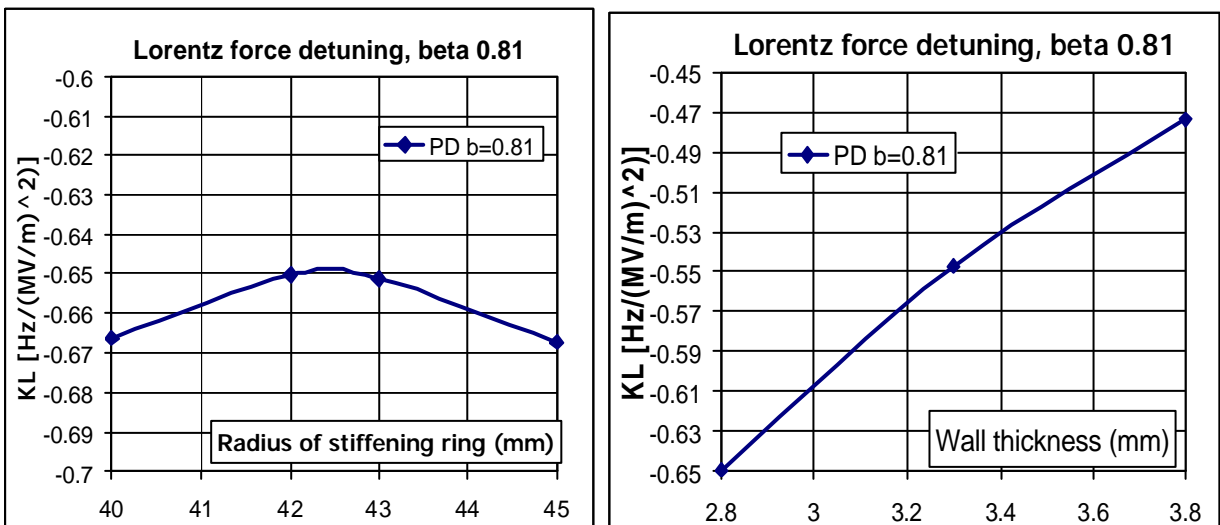


Fig.14. Detuning vs. position of the stiffening ring (left) and vs. cavity wall thickness (right).

Next picture in Fig.15 presents displacement distribution for three different position of the stiffening ring, including optimal position (42.5mm). Stress in niobium is shown in bottom right picture.

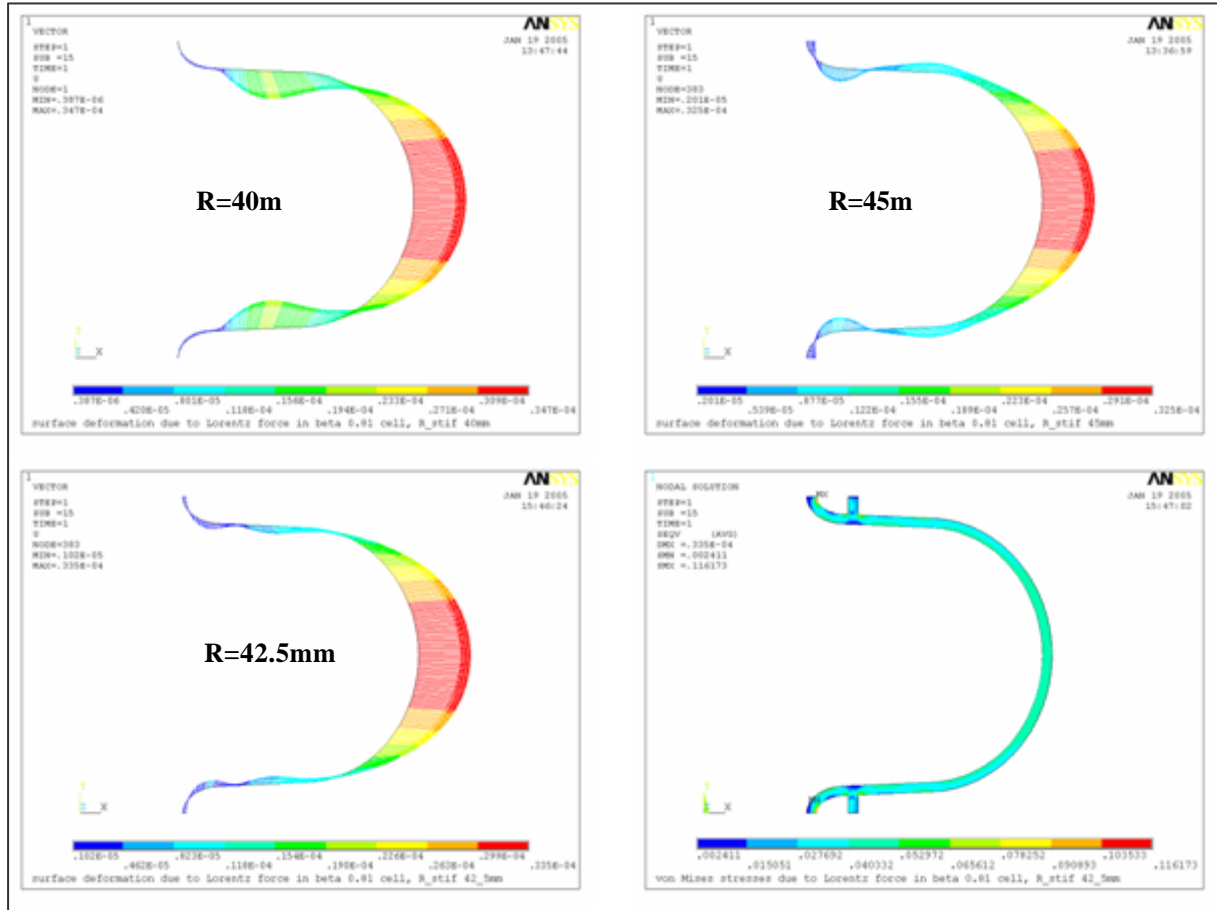


Fig.15. Vector of displacement for different position of the stiffening ring. Geometry and stress in niobium is shown in bottom right angle.

BETA 0.81, wall thickness 2.8mm				
DF(without ring)=- 982.9Hz for 25 MV/m				
R (mm)	40	42	43	45
DF (Hz) for 25MV/m	-416.5	-406.3	-406.9	-416.9
KL [Hz/(MV/m)^2]	-0.6664	-0.65008	-0.65104	-0.66704
Optimal ring position ~42.5mm				
Thickness (mm)	2.8	3.3	3.8	
DF (Hz) for 25MV/m	-406.1	-342.2	-296.2	
KL [Hz/(MV/m)^2]	-0.64976	-0.54752	-0.47392	

TTF 1.3 GHz cavity KL= -0.74 Hz/(MV/m)^2

SNS 0.8 GHz cavity KL= -0.7 Hz/(MV/m)^2

Lorentz detuning for squeezed LL cavity made of 2.8mm niobium is smaller than for TESLA and SNS cavity (wall thickness 3.8mm). The further decreasing of cavity detuning by using additional stiffening ring at equator area give only small improvements as shown in Fig. 16.

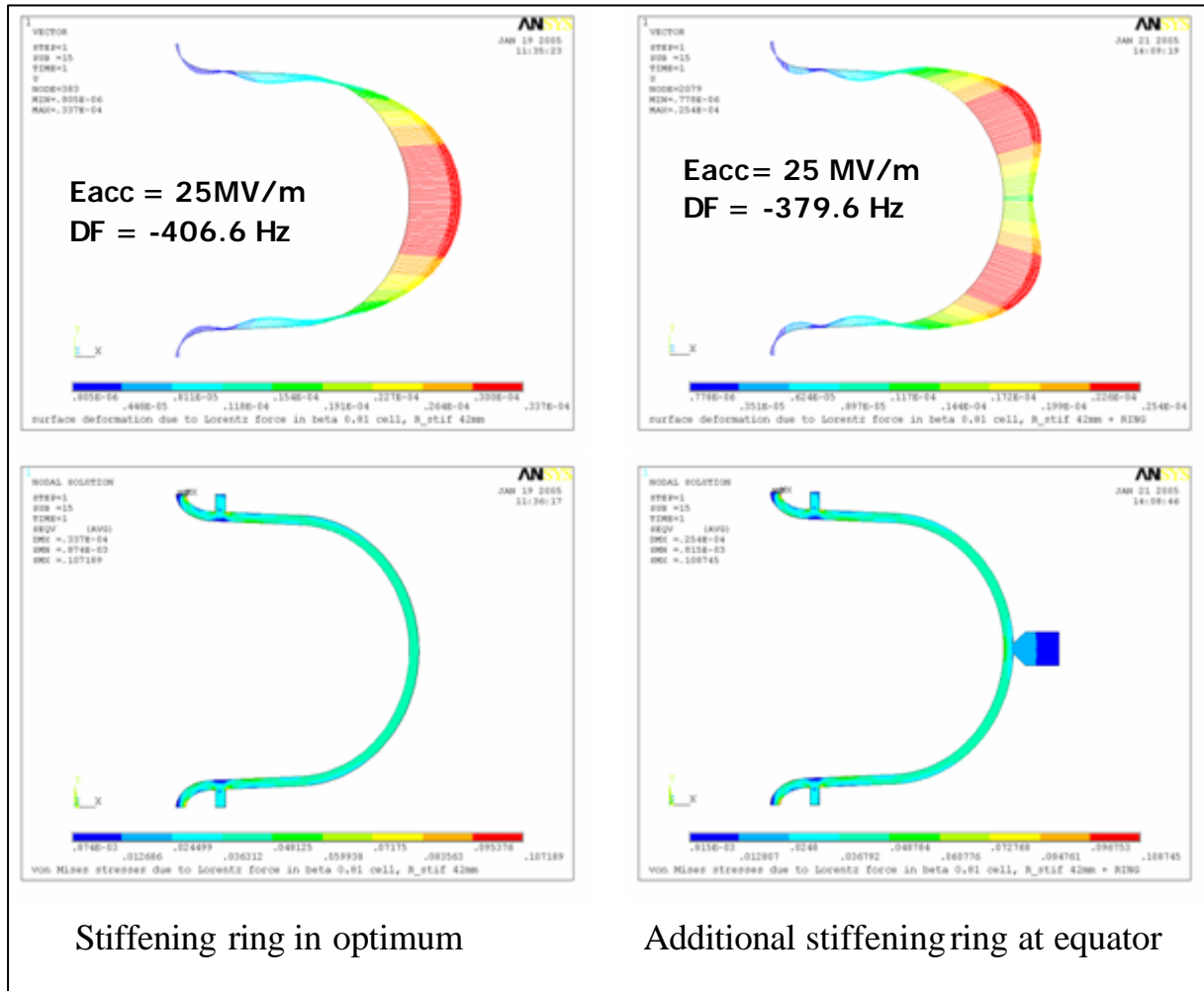


Fig.16. Cavity detuning and stress for LL squeezed cavity with standard stiffening ring (left) and additional radial stiffening ring, installed at equator (right).

Conclusion

Preliminary studies of two different designs for squeezed elliptical cavity with $b=0.81$ SNS-scaled cavity and Low Losses cavity shows that both designs will work for the Proton Driver, but LL design has more advantages: lower surface magnetic field and higher cell-to-cell coupling. This is important for 8cell cavity. End-tube assembly for LL cavity assumed the same as for the TESLA cavity. Lorentz forces for LL is smaller that for TESLA cavity. HOM analysis didn't show trapped modes with high R/Q. Need more studies and optimizations to accept design.

References:

1. G.W. Foster, M, Proton Driver Machine Overview and Main Linac, presented at FNAL Directors Review, March 15, 2005.